A handheld image-based gloss meter for complete gloss characterization

Stijn Beuckels[a], Jan Audenaert[a], Pierre Morandi[b], Frédéric B. Leloup[a]; [a]Light&Lighting Laboratory, KU Leuven (ESAT), BE-9000 Ghent, Belgium; [b]Rhopoint Instruments ltd., St. Leonards TN38 9AG, United Kingdom

Abstract

Nowadays, industrial gloss evaluation is mostly limited to the specular gloss meter, focusing on a single attribute of surface gloss. The correlation of such meters with the human gloss appraisal is thus rather weak. Although more advanced image-based gloss meters have become available, their application is typically restricted to niche industries due to the high cost and complexity. This paper extends a previous design of a comprehensive and affordable image-based gloss meter (iGM) for the determination of each of the five main attributes of surface gloss (specular gloss, DOI, haze, contrast and surface-uniformity gloss). Together with an extensive introduction on surface gloss and its evaluation, the iGM design is described and some of its capabilities and opportunities are illustrated.

Introduction

The human visual system effortlessly assesses the appearance of the materials that surround us. One of the main appearance attributes is gloss. Amongst other attributes such as colour and translucency, the gloss impression of surface finishes highly influences our product and quality judgements, and accordingly our purchase decisions. In this sense, manufacturers from various industries benefit from optical characterizations of the glossiness of their end products. Such optical evaluations of perceived glossiness are not straight-forward, partly because the dimensionality of the visual gloss appraisal is not fully understood yet. Based on an initial framework, the authors of this study presented five main attributes for the optical characterization of surface gloss [1]: specular gloss (perceived brilliance of the specular reflected highlights), DOI (Distinctness Of the reflected Image), haze (semi-specular reflection adjacent to the reflected images), contrast (contrast between specular reflecting areas and adjacent areas) and surface-uniformity gloss (texture, gloss unevenness or non-uniformities across the surface). These attributes are briefly illustrated in Figure 1.
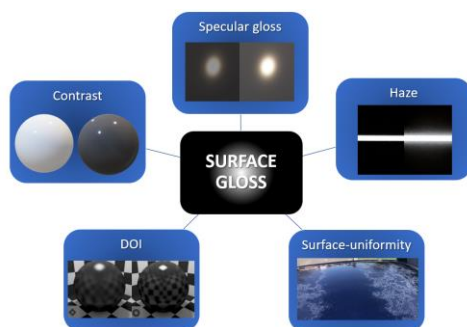

Figure 1. Five attributes of glossiness. (DOI-images from [2])

In general, the industrial quality control of glossiness is restricted to the measurement of the reflected flux in standardized measurement geometries by aid of the widely available and popular handheld specular gloss meter. Nowadays however, more sophisticated portable instruments have been introduced in the market for a more complete evaluation of glossiness. The Rhopoint IQ (Gloss-Haze-DOI meter) and Canon RA-532H (Surface Reflectance Analyzer) are examples of gloss meters that - besides specular gloss - measure surface reflectance profiles and standardized metrics for DOI and haze. More dedicated and expensive instrument examples are the Rhopoint TAMS and BYK-Gardner Spectro2Profiler, whose application is limited to specific niche industries. These instruments characterize surface relief maps and metrics for high gloss and low-gloss (textured) surfaces, resp. The current study focuses on the design and development of such an advanced - but more affordable, comprehensive and generally applicable - instrument with camera sensors for the characterization of metrics for each gloss attribute. The instrument complies to the specular gloss meter standards ([3],[4]), which is considered as an essential backward compatibility with traditional gloss meters. At the same time it captures more advanced measurements relevant to many industrial applications. It is an extension of a previously designed image-based gloss meter (iGM, such as presented in [5] and [6]), which processes the captured reflected light source image to evaluate new metrics for the attributes DOI, haze and contrast.[6] Sample measurements illustrated the versatility and utility of the system for several materials, including anisotropic surfaces. However, the device did not yet include any surface imaging, making the evaluation of surface-uniformity gloss (fifth gloss attribute) impossible. Furthermore, surface images can provide crucial information on the root cause of gloss deviations. Accordingly, an extended iGM instrument is described in this work with a surface imaging camera. The optical design is presented and illustrations of example measurements on various automotive panels are discussed.
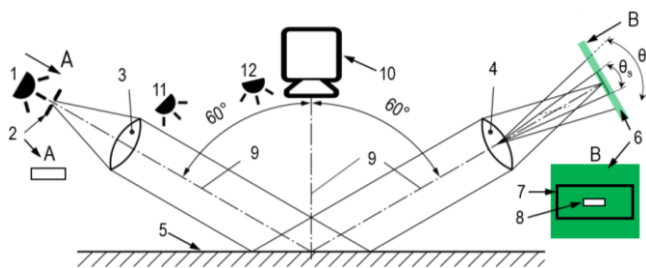
Gloss meter design

Image-based gloss meter

The iGM instrument designed in this study is summarized in Figure 2. It is based on the earlier design from Ref. [6], extended with a 0° camera (item 10) and several light sources at 45° and 10° angles of incidence (items 11 and 12). This extended iGM device complies to the widely known standards for a parallel beam 60° specular gloss meter ([3],[4]). It captures the reflected image of the (rectangular) light source aperture (item 2) with a 5MP colour CMOS sensor at 60° (item 6).

Via image-processing of the captured images in this 60°:60° geometry, the evaluation of specular gloss, DOI, haze and contrast (gloss) was illustrated in earlier work.[6],[7] The green channel of a measurement is shown in Figure 3a for a partially polished black glass sample of 75 GU (60°) with a high reflection haze. The according iGM metrics for each attribute are summarized in Table 1 and illustrated in Figure 3. Figure 3b&c display parallel and perpendicular signal lines, which are the reflection profiles in the parallel and perpendicular reflection planes (vertical and horizontal "line" from Figure 3a), resp. The specular gloss under 60° (denoted *SGU 60*), was quantified by

integrating the captured signal within the receptor field stop region (region 1). The *iGM specular luminance* was defined as the average signal over a number of highlight pixels within region 2. It is proportional to the luminance of the reflected source aperture image. For the characterization of DOI, the *iGM slope sharpness* was introduced as the mean of the two steepest slopes in the normalized parallel signal line. By way of example, these slopes are indicated as dotted lines in Figure 3b. The *iGM Haze* was calculated as the integrated signal in the large off-specular regions 3, relative to the integrated signal for a reference sample within region 1. This method resembles the standardized measurement method for reflection haze in the 20° or 30° geometry.[8] In addition, the *iGM Michelson contrast haze* (*iGM MC haze*) was put forward as a new haze metric. It is measured as the Michelson contrast between the highlight signal in region 5 and close off-specular signal in regions 4 (Figure 3a&b). Previously, standards for DOI and haze have been solely considered in the parallel reflection plane.[8],[9] With the 2D CMOS sensor, perpendicular surface characteristics – a perpendicular *iGM slope sharpness, haze* and *MC haze* - could now also be evaluated in the perpendicular direction, which is illustrated for the *iGM slope sharpness* and *MC haze* (regions 6&7) on the perpendicular signal line (cf. Figure 3a&c). Such evaluations comprise a highly different measurement than obtained by rotation of a conventional instrument over 90°, and are especially useful when considering anisotropic materials.[6] Two global contrast metrics, based on the contrast between the highlight luminance (*iGM specular luminance*) and the sample background luminance, were also introduced in the device. The sample background luminance was formerly measured in the 0°:60° geometry with a light source at the 0° angle.[6] This source has been removed in this work, but the extended iGM can now simply measure the background luminance with the 10° light source instead. The *iGM contrast* was based on the psychometric contrast (Weber contrast) between the *iGM specular luminance* and the sample background luminance.[6] The *iGM Contrast Gloss* (*iGM CG*), based on the Contrast Gloss formula by Leloup et al. [10], could be determined after calibration of the device for absolute luminance measurement.[7]
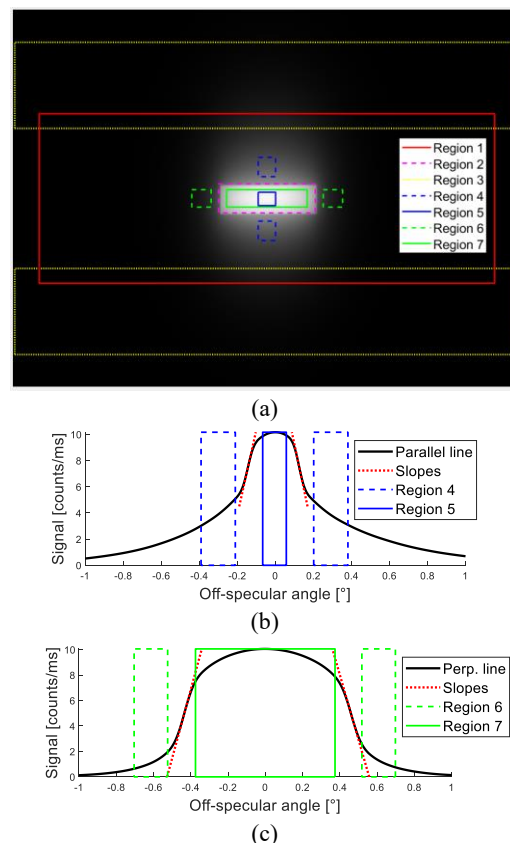
However there are disadvantages in using the standardized specular gloss meter geometry. Firstly, it measures an averaged effect over a fixed surface area illuminated with a collimated beam: rays passing through a single point of the source aperture create a parallel beam illuminating the whole measurement area on the surface, and are (for a perfectly flat surface) focused again on a single point on the CMOS sensor. As a result, there is no local distinction possible within the illuminated surface area, and only surfaces with locally uniform properties can be reliably measured. Secondly, the 60° CMOS sensor images solely the reflected source aperture image, and not the illuminated sample surface (the CMOS is in the focal plane of the receptor lens). Consequently, the instrumental conditions are vastly different than for example typical visual assessment conditions of surfaces (at reading distance). It is thus often impossible to assess the underlying physical causes of the measurement results. A reduction in the *iGM slope sharpness* could for example be caused by polishing traces, surface damage, sparkle, orange peel, surface texture, i.e. surface-uniformity gloss attributes (see illustrations in the measurements section).

Table 1. Metrics available in the iGM gloss meter

Spec. gloss	DOI	Haze	Contrast
- SGU 60 - Spec. lum.	- iGM slope sharpness	- iGM haze - iGM MC haze	- iGM contrast - iGM CG

(a)

(b)

(c)

Figure 3. iGM measurements of a hazy glass sample.

Figure 2. Schematic of the iGM gloss meter introduced in this work, based on ISO 2813 [3]. (1:specular source / 2:source aperture / 3&4:source & receptor lens / 5:sample surface / 6:60° CMOS / 7:receptor field stop region (θ_r) / 8: source aperture image (θ_s) / 9:optical axis / 10:0° CMOS with lens / 11&12:examples of 45° ring light and 10° point light)

It must be noted that there are numerous further options available for image-based metrics. Focusing on contrast-based metrics, one could for example use the sum of root-mean-squared (RMS) contrast of multiple band-passes of an image (see Schmid et al. or Storrs et al.[11],[12]), or the local band-limited contrast by Peli ([13],[14]), or Tadmor and Tolhurst their local contrast measure based on the Difference-of-Gaussian (DoG) of neurophysiological studies.[15]

Extended image-based gloss meter

As a solution to the described limitations, the iGM is extended with a 0° camera system. It is designed as a compromise between a large Field-of-View FoV (about 25 mm) and good image resolution of the sample surface. The theoretical

design of the extended system was optimized via simulations in TracePro. A lens diaphragm was added to improve the image quality (e.g. reducing the pincushion effect) and increase the Depth-of-Field (DoF). At the same time it however reduces the luminous flux to the sensor. Simulations were performed for multiple diaphragm diameters. The image quality, judged via the point spread function, was simulated as the sensor response for point sources on the sample surface at several distances from the optical axis. A diaphragm of 1 mm was selected, resulting in a DoF of approx. 1.5 mm (calculated with Eq. (22) from Ref. [16], using the sensor pixel pitch as Circle of Confusion).

Additionally, the design conditions were simulated for which the reflected image of a light source is visible on the 0° sensor (for a flat sample surface). The principle of reciprocity in optics was applied: the CMOS sensor was set to a Lambertian emitting light source and the sample to a flat reflecting mirror surface. The extend of the rays reflected by the surface was simulated for different distances above the sample. In addition, light sources should of course not interfere with the 60° gloss meter or the 0° camera system. As such, regions were obtained where a light source would have a reflected image inside or outside the sensor surface. A 45° ring light was introduced (reflected image outside the sensor), consisting of multiple LEDs evenly distributed on a circle and tilted towards the centre of the sample surface. In addition, another LED was placed at approx. 10° from the surface normal (denoted as 10° point light), with a reflected image on the 0° sensor. The usefulness of such visible and invisible light sources depends on the measurement application (see next section).

A prototype setup of this extended iGM was built in collaboration with a gloss meter manufacturer (Rhopoint Instruments Ltd.). All light sources can be individually powered. The camera sensors are connected to Matlab 2021 and controlled with a custom made Matlab application.

Measurements and discussion

The 0° camera system introduces new opportunities for image processing and the evaluation of surface-uniformity gloss metrics. Surface-uniformity gloss is roughly subdivided into three categories: surface texture (subdivided into physical texture - physical periodic structures on a surface – and optical texture - optical effect of reflective flakes inside coatings with a transparent top layer); gloss unevenness (non-uniformities across the surface due to material damage, scratches…); and orange peel (surface irregularity resembling the skin of an orange). An evaluation of each of them is now illustrated on some automotive interior and exterior surfaces.

Texture

Physical texture can be extracted from the 3D topography of surfaces.[17] For this purpose, images are captured with each of the 45° ring light LEDs separately activated. A surface height map is obtained via the "Shape from Shading" processing technique. It uses the shading in each image due to the directional illumination to reconstruct a 3D surface shape.[18] As an illustration, a textured automotive dashboard surface is measured with the iGM. Its 3D shape is reconstructed in Python using the procedure in Ref. [19]. An iGM measurement image with one of the LEDs is shown in Figure 4a. The reconstructed surface map is displayed in Figure 4b. Further pre-processing corrections for vignetting and radial distortion effects could still be applied to improve the uniformity of the result within the FoV.

Optical texture is illustrated on a dark blue coated automotive exterior surface. The sample consist of a metal base plate with multiple paint layers and a transparent top coat. It exhibits sparkle, caused by metal flakes inside the coating introducing bright spots at surface positions varying with the angle of viewing.[20] An example iGM measurement image is presented in Figure 4c&d for the 60°:60° specular gloss meter geometry and the 45°:0° geometry, resp. The sparkle is not visible in the 60°:60° geometry (due to the beforementioned averaging over the illumination spot). Solely a small off-specular haze signal is detected at increased exposure time. In turn, the 45°:0° measurement clearly reports the individual sparkle spots. Ferrero et al. proposed two dedicated metrics for sparkle from such measurement images: sparkle visibility (based on the contrast between sparkle spots and their surround) and sparkle density (number of visible spots per square mm).[21]

Gloss unevenness

For the illustration of gloss unevenness, the same dark blue automotive panel is post-processed with a rotary polisher using heavy cut polish compound. As a result, the surface is scratched and shows – besides sparkle - polishing effects, such as swirls (circular scratches) and holograms (ghost-like streaks observed with a small bright light source, such as the sun).[22] A picture of the resulting surface, illuminated with such a bright light source, is shown in Figure 4e with annotations of the different effects. Measurement images in the 60°:60° geometry are given in Figure 4f, indicating a pronounced directional haziness at increased exposure time. The direction of the haziness - diagonal in this example – changes according to the orientation of the device relative to the scratches or swirls. Conventionally, haziness is only evaluated in the parallel reflection plane (vertical direction), thus requiring careful orientation of the device for representative measurements. The image data and camera preview of the iGM can ease this orientation process, which is certainly non-trivial for samples with such severe position-dependent directionality. The 0° camera image, on the contrary, distinguishes the scratches, swirls and holograms clearly with the 10° point light (Figure 4g) and with the 45° ring light (Figure 4h). They appear as thick lines or curves, thin concentric circles around the light source, and long stretched highlight regions starting at the light source, resp. A separate detection should thus be possible from these measurement images via thresholding, edge detection, image segmentation, shape recognition, machine learning methods, etc. Further details are however outside the scope of this work. The authors refer to Sonka et al. for various possibilities.[23]

Orange peel

Orange peel is caused by smooth bidirectional variations of the surfaces profile with certain spatial frequencies giving it the appearance of the peel of an orange. This effect is often caused by gravity effects during a spray painting process. It is typically measured by analysing the Fourier spectrum of reflected profiles within specific wavelength ranges. Its evaluation with the iGM is illustrated with the Orange Peel Standard set from ACT Test Panel Technologies.[24] This sample set contains ten coated metal plates from severe orange peel (panel 1) to absence of orange peel (panel 10). Example images for panel 1, 5 and 10 in the 60°:60° geometry are given in Figure 4i (left images). These images do not show the typical spatial frequency effect of orange peel. Due to the beforementioned averaging over the illuminated surface, the orange peel only influences the sharpness of the

reflected source aperture image. For a relevant characterization of orange peel, however, the deformation of a long light source edge – such as a masked light source or a filament LED source - through reflection on the surface should be determined. This is also not possible with the invisible 45° ring light or the small 10° point light. In order to imitate such a required light source, a thin white plastic ring is placed in the iGM (at approx. 20° angle around the 0° angle). This ring illuminated by the 45° ring light, making its reflection visible on the 0° sensor. The resulting sensor images are shown in Figure 4i, illustrating the visibility of the deformation due to orange peel. In fact, orange peel could now be evaluated from Fourier analysis of the deformation of the edges from their original circular shape. Sone et al. presented such a method for a reflected linear edge and defined "Orange peel noise" as a metric for the orange peel effect.[25]

Conclusion

In this work, an image-based gloss meter (iGM) incorporating two colour CMOS cameras was described. The instrument is capable of evaluating each of the five main attributes of surface gloss: specular gloss, DOI, haze, contrast and surface-uniformity gloss. While a former design of the instrument dealt with the first four attributes, the surface-uniformity evaluation was added via imaging of the sample surface. Opportunities for characterizing 3D texture, sparkle, surface defects, and orange peel were illustrated with the device on automotive panels, by using multiple light sources such as LEDs on a 45° ring, a point light at 10° angle and an imitation of a circular light source at 20°. Future research is to be performed on other materials, together with the development of case-specific image processing methods and metrics. Furthermore, none of the presented opportunities are currently using the available spectral differentiation between the colour channels (RGB) of the sensors. Finally, there are other aspects of glossiness that were not considered in this study. For example the evaluation of sheen (the specular gloss at grazing reflection angles, typically 85°) or graininess (the visibility of material grains under diffuse illumination) would require additional hardware extensions of the current iGM.[1],[20]
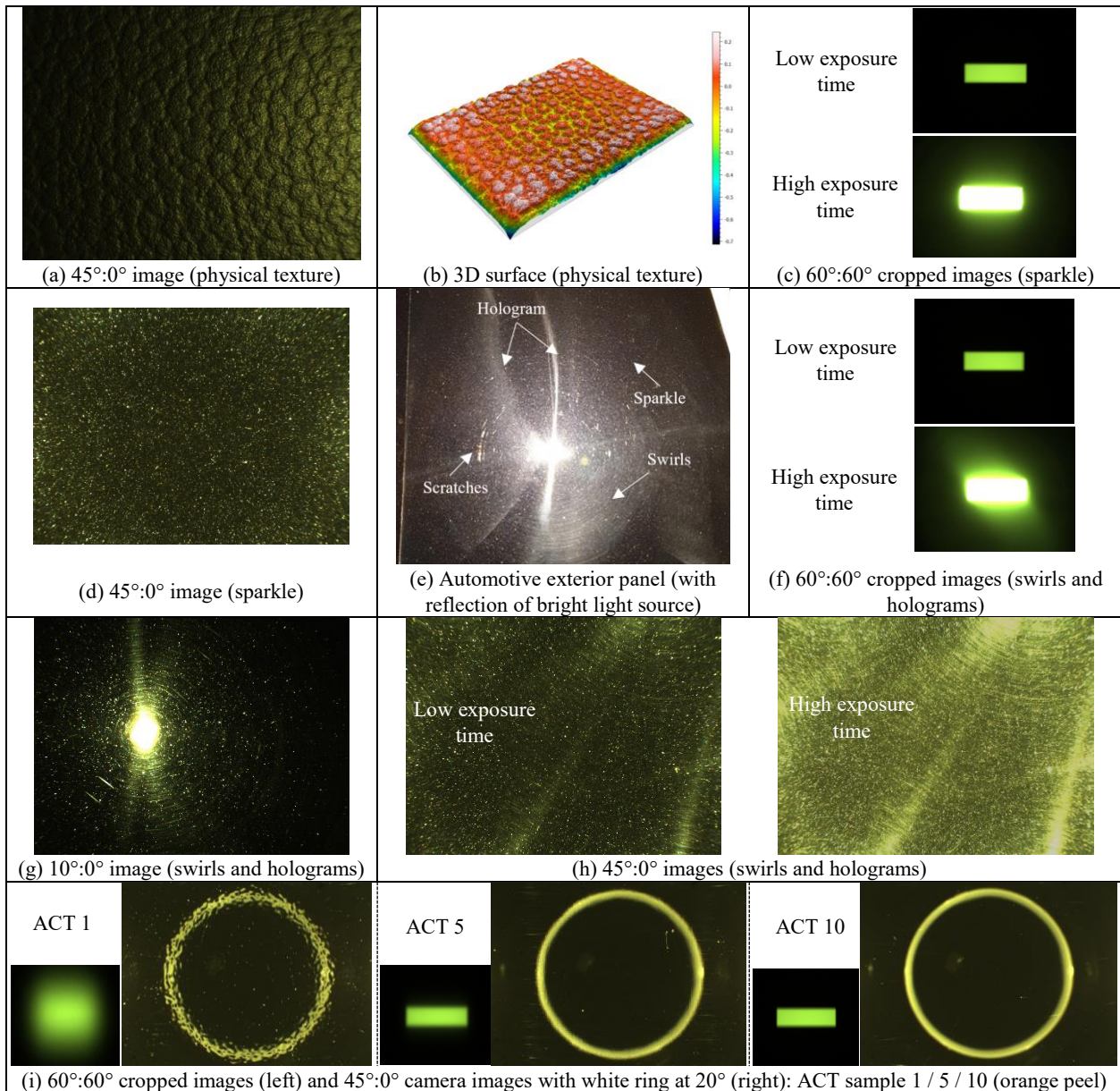

(a) 45°:0° image (physical texture)

(b) 3D surface (physical texture)

(c) 60°:60° cropped images (sparkle)

Low exposure time

High exposure time

(d) 45°:0° image (sparkle)

(e) Automotive exterior panel (with reflection of bright light source)

(f) 60°:60° cropped images (swirls and holograms)

Low exposure time

High exposure time

(g) 10°:0° image (swirls and holograms)

(h) 45°:0° images (swirls and holograms)

Low exposure time

High exposure time

ACT 1

ACT 5

ACT 10

(i) 60°:60° cropped images (left) and 45°:0° camera images with white ring at 20° (right): ACT sample 1 / 5 / 10 (orange peel)

Figure 4. Evaluation examples for surface-uniformity gloss on automotive interior and exterior surfaces.

References

[1] R. S. Hunter, "Methods of determining gloss," *J. Res. Natl. Bur. Stand. (1934).*, vol. 18, no. 1, p. 19, 1937, doi: 10.6028/jres.018.006.

[2] J. A. Ferwerda, F. Pellacini, and D. P. Greenberg, "Psychophysically based model of surface gloss perception," *Hum. Vis. Electron. Imaging VI*, vol. 4299, pp. 291–301, 2001, doi: 10.1117/12.429501.

[3] ISO, *ISO Standard 2813 (2014): Paints and varnishes — Determination of gloss value at 20°, 60° and 85°*. International Organization for Standardization, 2014.

[4] ASTM, *ASTM D523 - 14 (2018): Standard Test Method for Specular Gloss*, no. Reapproved 2018. American Society for Testing and Materials, 2018.

[5] F. B. Leloup, J. Audenaert, and P. Hanselaer, "Development of an image-based gloss measurement instrument," *J. Coatings Technol. Res.*, vol. 16, no. 4, pp. 913–921, 2019, doi: 10.1007/s11998-019-00184-8.

[6] S. Beuckels, J. Audenaert, P. Hanselaer, and F. B. Leloup, "Development of an image-based measurement instrument for gloss characterization," *J. Coatings Technol. Res.*, vol. 19, pp. 1567–1582, 2022, doi: 10.1007/s11998-022-00630-0.

[7] S. Beuckels, J. Audenaert, F. Leloup, and P. Hanselaer, "Contrast gloss evaluation by use of a camera-based gloss meter," in *Proceedings of SPIE (Unconventional Optical Imaging III)*, 2022, vol. 1213610, p. 8, doi: 10.1117/12.2621134.

[8] ASTM, *ASTM E430 - 19 (2019): Standard Test Methods for Measurement of Gloss of High-Gloss Surfaces by Abridged Goniophotometry*. American Society for Testing and Materials, 2019.

[9] ASTM, *ASTM D5767 - 18 (2018): Standard Test Methods for Instrumental Measurement of Distinctness-of-Image Gloss of Coating Surfaces*. 2018.

[10] F. B. Leloup, M. R. Pointer, P. Dutré, and P. Hanselaer, "Luminance-based specular gloss characterization," *J. Opt. Soc. Am. A*, vol. 28, no. 6, 2011, doi: 10.1364/JOSAA.28.001322.

[11] A. C. Schmid, P. Barla, and K. Doerschner, "Material category determined by specular reflection structure mediates the processing of image features for perceived gloss," *bioArxiv*, pp. 1–45, 2020.

[12] K. R. Storrs, R. W. Fleming, B. L. Anderson, and R. W. Fleming, "Unsupervised learning predicts human perception and misperception of gloss," *bioRxiv Neurosci.*, vol. 49, no. 0, May 2021, doi: 10.1101/2020.04.07.026120.

[13] E. Peli, "Contrast in complex images," *J. Opt. Soc. Am. A*, vol. 7, no. 10, pp. 2032–2040, 1990.

[14] P. J. Marlow, J. Kim, and B. L. Anderson, "The perception and misperception of specular surface reflectance," *Curr. Biol.*, vol. 22, no. 20, pp. 1909–1913, 2012, doi: 10.1016/j.cub.2012.08.009.

[15] Y. Tadmor and D. J. Tolhurst, "Calculating the contrasts that retinal ganglion cells and LGN neurones encounter in natural scenes," *Vision Res.*, vol. 40, no. 22, pp. 3145–3157, 2000, doi: 10.1016/S0042-6989(00)00166-8.

[16] J. Conrad, "Depth of Field in Depth," p. 45, 2006.

[17] A. Ramola, A. K. Shakya, and D. Van Pham, "Study of statistical methods for texture analysis and their modern evolutions," *Eng. Reports*, vol. 2, no. 4, pp. 1–24, 2020, doi: 10.1002/eng2.12149.

[18] E. Prados and O. Faugeras, "Shape From Shading," in *Handbook of Mathematical Models in Computer Vision*, Boston, MA, 2006, pp. 375–388.

[19] R. J. Woodham, "Photometric method for determining surface orientation from multiple images," *Opt. Eng.*, no. 19, pp. 139–144, 1980.

[20] C. S. McCamy, "Observation and measurement of the appearance of metallic materials. Part II. Micro appearance," *Color Res. Appl.*, vol. 23, no. 6, pp. 362–373, 1998.

[21] A. Ferrero *et al.*, "An insight into the present capabilities of national metrology institutes for measuring sparkle," *Metrologia*, vol. 57, no. 6, 2020, doi: 10.1088/1681-7575/abb0a3.

[22] C. Brown, "Common auto detailing paint defects and issues," 2023. [Online]. Available: https://www.ocdcarcare.com/auto-detailing-articles/common-auto-detailing-paint-defects/#Buffer_Trails_and_Holograms. [Accessed: 01-Mar-2023].

[23] M. Sonka, V. Hlavac, and R. Boyle, *Image processing, analysis, and machine vision*, Fourth. 2014.

[24] ACT Text Panel Technologies, "ACT Orange peel standard." .

[25] T. Sone and S. Watanabe, "Measurement and Evaluation Method of Orange Peel," in *Electronic Imaging, Material Appearance 2017*, 2017, vol. 2017, no. 8, pp. 62–65.

Author Biography

Stijn Beuckels received the degree of master of engineering in Energy at the KU Leuven (2014). He worked at TE Connectivity Belgium for five years as a product validation test engineer for automotive parts. Since 2020 he is performing a PhD on the optical metrology of perceptual surface glossiness at the Light&Lighting laboratory (KU Leuven). His research mainly focuses on the future of industrial surface gloss evaluation.

Jan Audenaert graduated as a master in information and communication technology from Katholieke Hogeschool (KAHO) Sint-Lieven (Gent) in 2009. He obtained his PhD in engineering from KU Leuven in 2014. Currently he is active at the Light&Lighting Laboratory as a research expert with a main research focus on ray tracing for non-imaging optics and near-field goniophotometry.

Pierre Morandi has 2 master degrees in Mechanical Engineering, Building Energy Efficiency Engineering and a PhD degree in mechanical and optical metrology (2014, Pprime Institute, Poitiers, France). Since that he has been leading the development of the Rhopoint TAMS™ instrument for Rhopoint Instruments Ltd. (UK). Pierre has worked for nearly 9 years in collaboration with major German automotive OEMs, to develop specific and innovative algorithms for painted surface finish quality control and 3D topographical analysis.

Frédéric Leloup received his MSc in Electromechanical Engineering in 2001 and PhD in Engineering in 2012, both from KU Leuven (Belgium). He worked as a research fellow and postdoc researcher at the Light&Lighting Laboratory research group, before being appointed associate professor in the Department of Electrical Engineering at KU Leuven in 2022. His research focuses on hard and soft lighting metrology. Frédéric is president of the Belgian Institute on Illumination and National Representative within CIE Division 1 (Vision and Colour).